JOURNAL
OF
GEOMAGNETISM
AND
GEOELECTRICITY

VOL. X NO. 2

SOCIETY
OF
TERRESTRIAL MAGNETISM AND ELECTRICITY
OF
JAPAN

1959
KYOTO

JOURNAL OF GEOMAGNETISM AND GEOELECTRICITY

EDITORIAL COMMITTEE

EDITORIAL OFFICE: Society of Terrestrial Magnetism and Electricity of Japan,
Geophysical Institute, Kyoto University, Kyoto, Japan

The fields of interest of this quarterly Journal are as follows:

Terrestrial Magnetism	Aurora and Night Airglow
Atmospheric Electricity	The Ozone Layer
The Ionosphere	Physical States of the Upper Atmosphere
Radio Wave Propagation	Solar Phenomena relating to the Above Subjects
Cosmic Rays	Electricity within the Earth

The text should be written in English, German or French. The price is set as 1 dollar per number.

The Editors

World-wide Distribution of Cosmic-Ray Neutron Intensity at Sea Level

By Masahiro KODAMA

The Institute of Physical and Chemical Research

(Read October 26, 1958; Received January 20, 1959)

Abstract

The world-wide distribution of cosmic ray intensity at sea level was decided from the several latitude surveys so far carried out by many researchers. The contour map thus obtained was compared with the various models for the earth's geomagnetic field.

§ 1. Introduction

Recently, the discussions relating to the effects of the earth's geomagnetic field for cosmic rays have opened again since the discrepancy between observed cosmic ray equator and the geomagnetic dipole equator was pointed out by Simpson (1956). There are two possible explanations for the geomagnetic field effective on cosmic ray particles. The one is due to the distortion of the geomagnetic field at large distances from the earth by conducting interplanetary gas. The other (Rothwell et al., 1957; storey, 1958) is due to the geomagnetic field which consists of both the dipole and non-dipole parts, or in other words, due to the geomagnetic local anomalies.

In order to asertain the above assumptions, it is natural in principle that one should give one's notice on the distributions of cosmic ray intensities not only along the equator or special longitudes but also over the world. Results of cosmic ray latitude surveys so far carried out by many researchers, therefore, must carefully be checked again from the synthetic point of view that put individual measurements together.

First, the world-wide distributions of cosmic ray intensities should be decided and then compared them with the various models for the earth's geomagnetic field which are supposed to be more effective for cosmic rays. Although lines of equal cosmic ray meson component at sea level were reported by Millikan and Neher (1936) about twenty years ago, it seems inadequate for the precise discussions on the present problem because meson components have the atmospheric temperature effect and its latitude effects are not so large. Second, when the cosmic ray intensity remarkably varied from day to day, for example, as a Forbush type decrease at the time of a magnetic storm, the study on the time variations of world-wide distributions may be useful for making clear the relationship between cosmic rays and the geomagnetic field.

In the present report, equal innensity lines of cosmic ray nucleonic components were obtained by using five latitude curves for nucleonic components and four for meson components. Then they were compared with the various models for the earth's

geomagnetic field. As regards to the second subject, it will be discussed in the following paper.

§ 2. List of data used for the analysis

So far, many surveys on latitude and longitude effects of cosmic rays have been carried out at sea level, or aeroplane altitude. But the data obtained at sea level only, as shown in Table 1, were used in the present analysis. Because it is not so simple to convert the results obtained at high altitude into that at sea level. Fig. 1 shows the

Table 1

Authors	Type of apparatus	Periods of survey	Solar activity
(1) Compton and Turner (1937)	ionization chamber	Mar. 1936–Jan. 1937	maximum
(2) Sekido, Asano and Masuda (1943)	ionization coamber	Apr. 1937–Mar. 1939	maximum
(3) Rose and Katzman (1956 ; 1956)	neutron monitor	Oct. 1954	minimum
(4) Simpson, Fenton, Katzman and Rose (1956)	neutron monitor	Dec. 1954	minimum
(5) Simpson, Fenton, Katzman and Rose (1956)	neutron monitor	Feb.–Apr. 1955	minimum
(6) Kodama and Miyazaki (1957)	ionization chamber and neutron monitor	Nov. 1956–Apr. 1957	maximum
(7) Rothwell and Quenby (1957)	neutron monitor	Feb.–May 1957	maximum
(8) Law, Mckenzie and Rathgeber (1949)	counter telescope	July–Aug. 1948	maximum

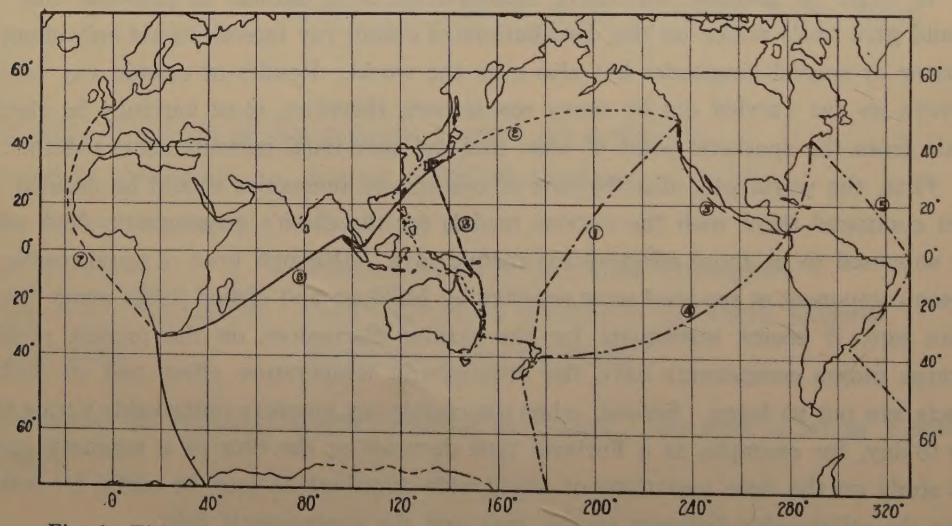

Fig. 1 The voyage courses on which cosmic ray measurements were carried out.

respective routes along which cosmic ray measurements were made. Numbers attached to each routes correspond to that in Table 1. The reason why meson components were

adopted is mainly owing to the fact that there is few latitude surveys for nucleonic components on the Pacific Ocean.

§ 3. Normalization of data

Measurements shown in Table 1 were performed by using the various type or different size of apparatus in their respective surveys. Accordingly, it is necessary to be normalized the observed values so that the direct comparison becomes possible each other for the purpose of making a contour map for cosmic ray intensity. The observed values of cosmic ray intensities usually are represented by the counted numbers per unit time. In order to investigate the remarkable intensity variations such as latitude effects, it is proper to utilize the logarithmic representation (Wada, 1957) of the counted number, because a percentage of the intensity changes with the value of the mean intensity adopted. However, the direct comparison of the latitude curves thus obtained is impossible without normalization among each other. It was performed as follows.

When the individual surveys passed through the same location on their way, the obtained data were normalized to the same absolute intensity at its location. For example, Tokyo is a normalization point between (2) and (6) shown in Table 1 and also Cape Town is that between (6) and (7). In that case, it must be considered on the secular variation of cosmic ray intensity. Although the so-called eleven year cycles for cosmic rays has been reported by Forbush etc., all of them are being observed at one location on the earth's surface and no observations were made regarding the change of latitude curve along the same course in different years. As the first approximation, therefore, we do not consider the secular variation till the discussion in § 5.

Next, in order to convent the latitude curve observed for meson components into that for nucleonic components, results for both components in (6) were improved, where the ratio of the nucleonic component to the meson component, corrected for the barometric pressure respectively, was 4.3 for the total change of latitude effects. We assumed the new curve multiplied the latitude curve for the meson component by factor 4.3 to be the one for the nucleonic component.

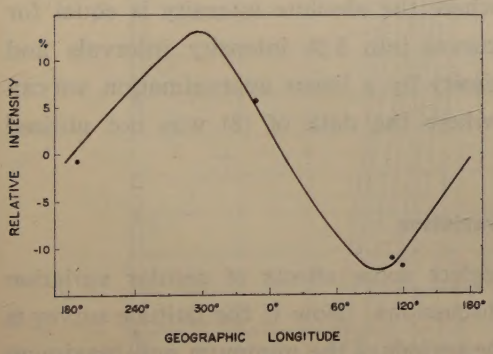

Fig. 2 The longitude effect for the nucleonic component at cosmic ray equator. Each points and a solid line represent the results obtained at sea level and 18,000 feet, respectively.

The results of observations were divided into two groups, i.e. group I–1, 2, 6, 7 and group II–3, 4, 5. The normalization among these two groups was made by using the different method as follows. Studying the change of the minimum intensities in each latitude curves against the geographic longitude for group I, it is evident from Fig. 2 that all of the minimum intensities in four curves completely fit with the longitude curve obtained at 18,000 feet along cosmic ray equator by Simpson (1958). Therefore, we tried to normalize group II into group I

so that the minimum intensities of each curves for group II may fit with a Simpson's curve. The reason why the above method adopted is due to little effect of secular variations of cosmic ray intensities at lower latitudes. Moreover, it is due to the fact that if the above method is not adopted, the normalization among both groups is obliged to be done at Vancouver located in high latitude where there is no data of nucleonic components in group I. In this ways, all of available latitude curves were arranged into those normalized by the absolute intensity, as shown in Fig. 3.

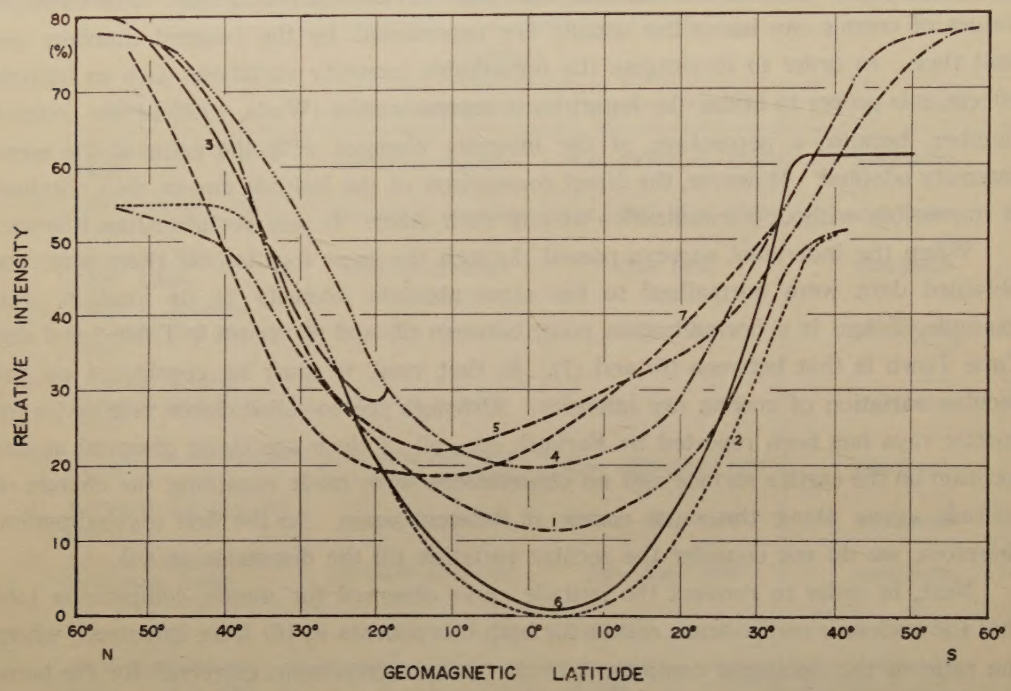

Fig. 3 The latitude curves normalized with each other.

§ 4. Contour map

We can decide from Fig. 3 the positions where the absolute intensity is equal for different latitude curves. By dividing each curves into 5 % intensity intervals and then connecting the positions of the equal intensity by a linear approximation, we can obtain a contour map of cosmic rays, Fig. 4, where the data of (8) was not utilized for its route is close with (2).

§ 5. Secular variation

As mentioned in § 3, it is impossible to neglect some effects of secular variation in cosmic ray intensity for the more precise discussions. Now if the latitude survey is carried out along the constant course twice at the periods of the minimum and maximum solar activity, the expected result probably is as shown in Fig. 5, where the difference between the intensity for the solar minimum and that for the maximum increases as the latitude becomes higher and also the position of latitude knee for the minimum shifts

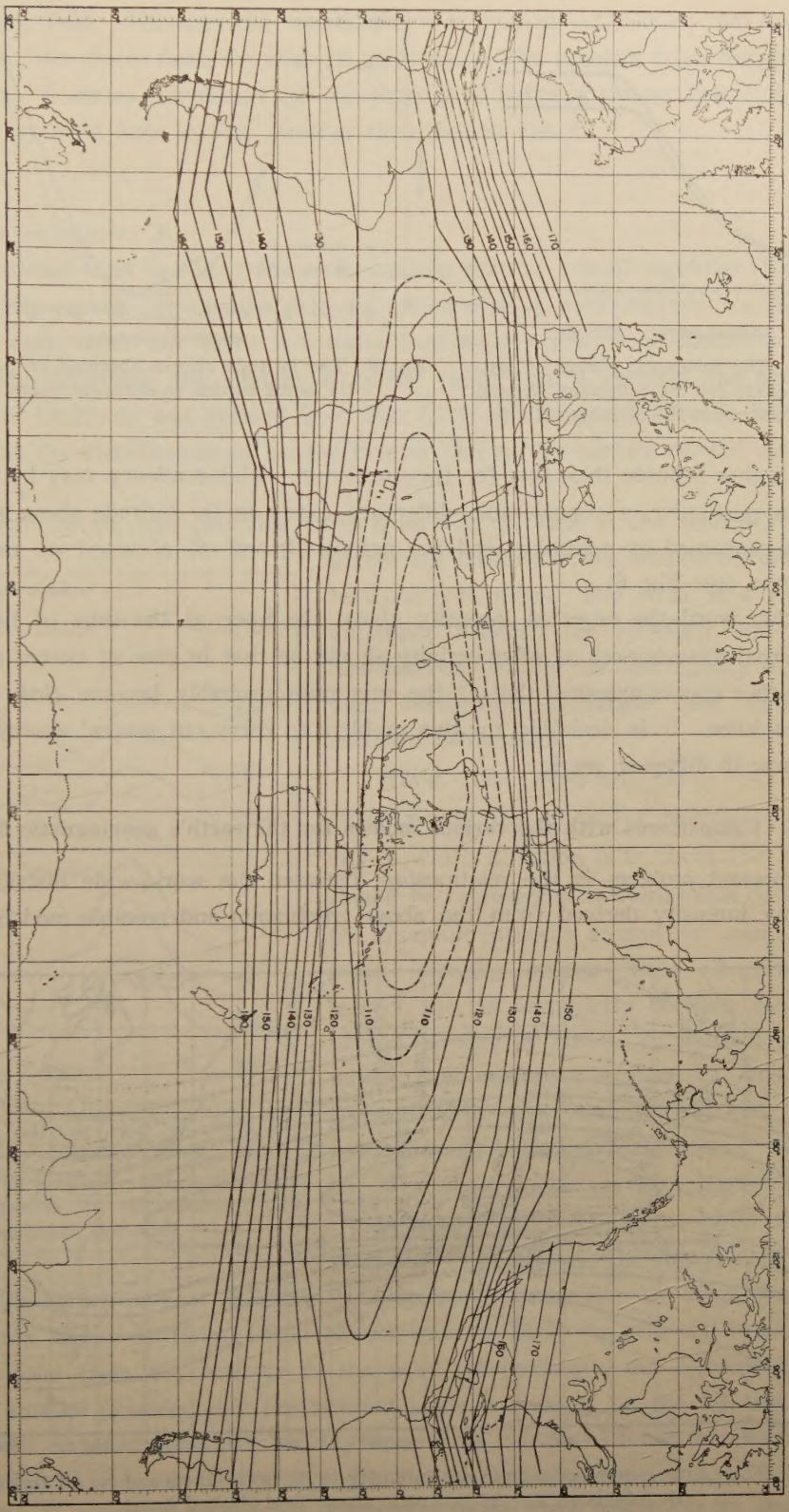

Fig. 4 The contour map of cosmic ray intensity.

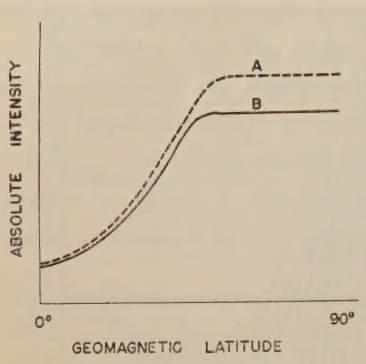

Fig.5 The schematic curves of latitude effect for the minimum (A) and the maximum (B) of solar activity.

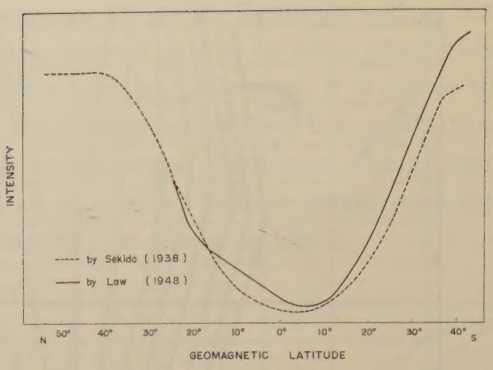

Fig. 6 The latitude curves obtained on nearly the same course in different years.

towards higher latitude than that for the maximum. This tendency may be found in Fig. 3, in particular, a considerable difference exists at the latitude above the knee. This was confirmed by a similar tendency among (2) and (8) obtained on nearly the same course. (see Fig. 6)

In other words,the expected intensity above the knee at the time of having no such external disturbances as solar activity should be that in case of curves (3), (4) or (5), and other curves excepted that at the minimum probably become close to them above the knee. It is desirable for this problem to carry out several surveys on the same course in different years.

§ 6. Comparisons with the various models for the earth's geomagnetic field

The present problem is the relationship between the world-wide distribution of cosmic ray intensity derived from the above treatments and possible models for the

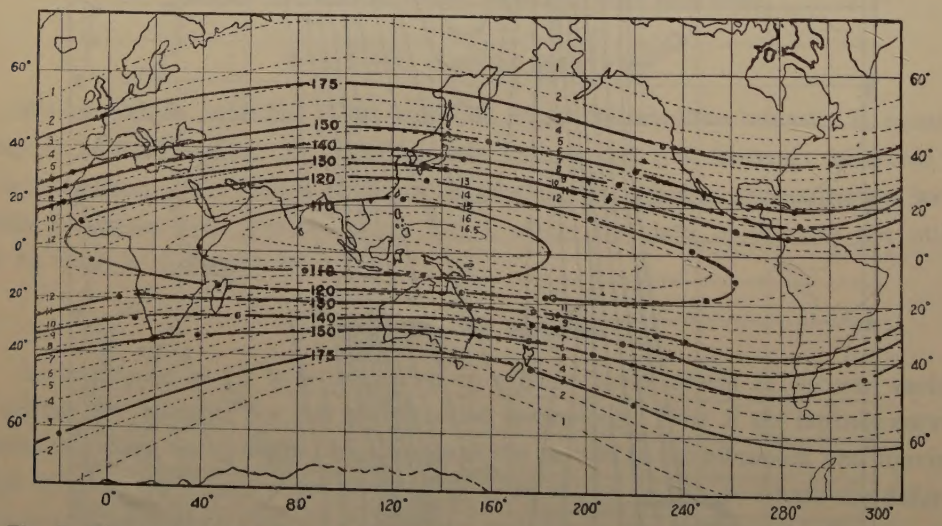

Fig. 7 The contour maps of cosmic ray intensity in % (solid lines) and cut-off rigidity in Bv calculated for the eccentric dipole field (dashed lines).

geomagnetic field. Although the discrepancy was pointed out already on cosmic ray equator for the dipole field, we wish to judge again this problem from the world-wide standpoint. It seems convenient for our purpose to make a contour map smoothed up as shown by solid lines in Fig. 7 rather than that in Fig. 4.

a). *Eccentric dipole : F_e*

The dotted lines in Fig. 7 show the contour map of cut-off rigidities (Kodama et al., 1957) for cosmic ray calculated in F_e. At a glance, both contour maps seem to resemble each other but there is a siginificant difference between them. In order to find out the difference, the change of cut-off rigidity on a contour line against the geographic longitude was derived from Fig. 7. If this longitude effect is neglected, it means that the distributions of cosmic rays on the earth's surface depend only on the effect of F_e.

We can obtain two probable facts from Fig. 8. One is the tendency that the higher the latitude is, the smaller the discrepancy between both maps. The other is a siginificant difference between the northern and southern hemissheres, or, that the discrepancy in the southern hemisphere is larger than that in the northern hemisphere.

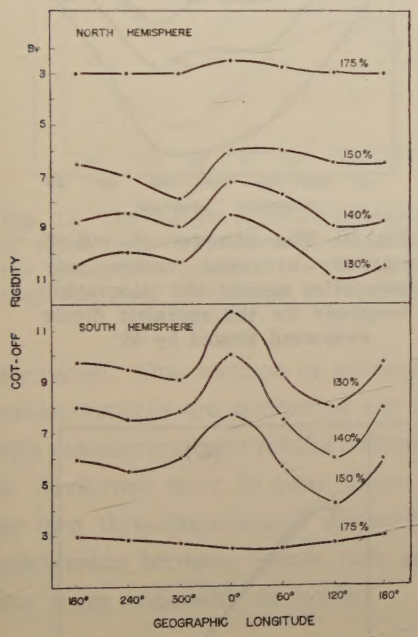

Fig. 8 The longitude effects of cosmic ray intensities at the constant geomagnetic latitudes.

While, the expected curve of longitude effects due to the fact for the geomagnetic eccentricity of which direction is in about 150° longitude should be represented as a sinusoidal curve having the minimum intensity around 150° and the maximum intensity around 330°. Regarding this subject, too, an asymmetry between both hemispheres is found in Fig. 9. In summary, a simple model of F_e could not explain not only the discrepancies on each locations but also the differences among both hemispheres.

b.) *West-ward shifted eccentric dipole : F_s*

In case of the dipole field rotated 45° to west proposed by Simpson, the figure corresponding to Fig. 8 is shown in Fig. 10 where the discrepancy becomes more large than that in case a) for higher latitudes. This phenomenon is likely to arise from an uniform rotation done from the equator to the poles. Accordingly, the discrepancy maybe becomes smaller provided that the rotation angle is reduced as the latitude becomes higher. As an example, three rigidity spectrums calculated for Rose's data (3) were shown in Fig. 11 (A) and (B) correspond to F_e and F_s, respectively, and (C) corresponds to the field of which rotation angle represented by $45° \cos\lambda$, where λ is the geomagnetic

latitude. These facts suggest that the distortion of the geomagnetic field at large distances from the earth may not be uniform but tortuous.

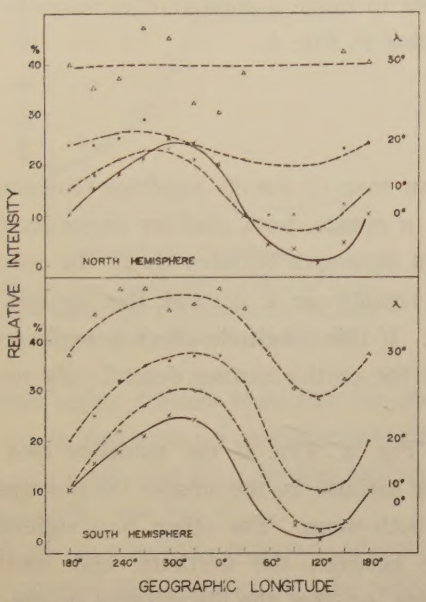

Fig. 9 The changes of cut-off rigidities of equal cosmic ray intensities against the geographic longitude for the eccentric dipole.

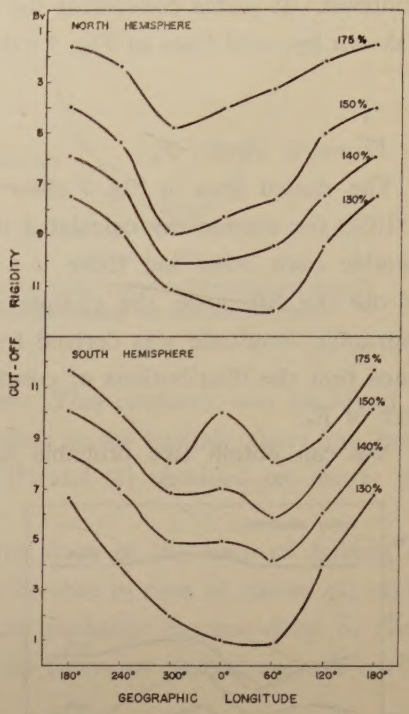

Fig. 10 The changes of cut-off rigidities of equal cosmic ray intensities against the geographic longitude for the eccentric dipole west-ward shifted by 45°.

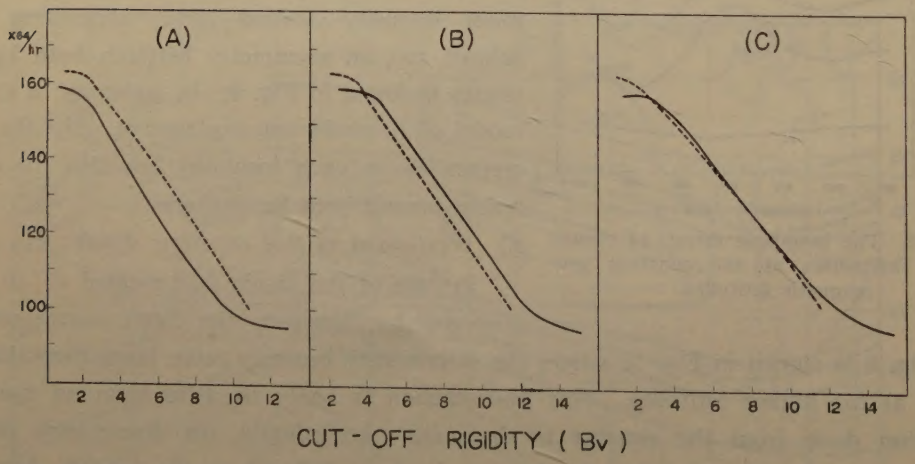

Fig. 11 The change of cosmic ray intensity against the cut-off rigidity for Rose's latitude survey. Solid and dashed lines represent the results on the Pacific Ocean and the Atlantic Ocean, respectively. The cut-off rigidities were calculated for (A) eccentric dipole, (B) eccentric dipole west-ward shifted by 45° and (C) eccentric dipole west-ward shifted by 45° cos λ.

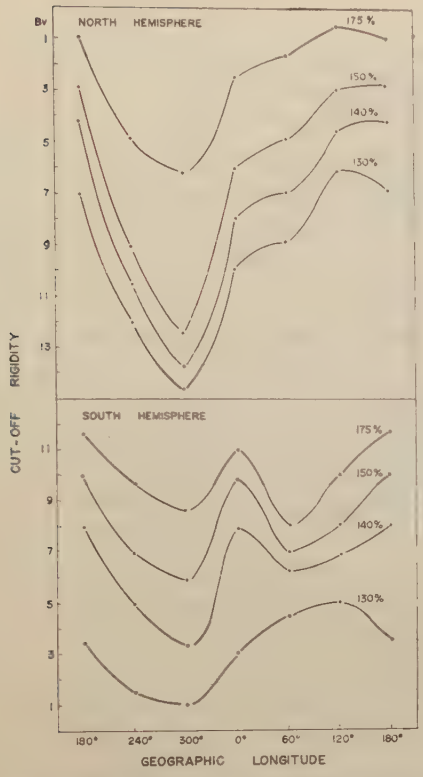

Fig. 12 The changes of cut-off rigidities of equal cosmic ray intensities against the geographic longitude for the geomagnetic field calculated by Quenby and Webber.

c). Non-dipole field

Quenby and Webber (1958) especially noticed to the non-dipole parts and calculated the field contains from 1st to 6th term for the spherical harmonic representation of the geomagnetic field. It will be seen from Fig. 12 that the discrepancy in that case is larger than those in the previous cases. Considering the physical means relating to this assumption, it is rather difficult to suppose that the higher order parts of the geomagnetic field are predominant at a large distance from the earth. On the other hand, the recent experimental results (Rothwell et al., 1957; Oguti et al.,) show that a close relationship exists between cosmic rays and the geomagnetic local anomalies. It may be, therefore, most useful to study cosmic rays at sea level or high altitude around the local anomalies.

Although the discussions has been made on the various models for the earth's geomagnetic field, no sufficient explanation has come out for the world-wide distributions of cosmic ray intensities. One method of solving the present problem is that the more detailed and precise surveys are performed not only on cosmic rays but also on the geomagnetic field with considering their secular variations. In results of the rocket experiments which will be developed more in near future will bring the two-dimensional discussions done so far into three-dimensional discussions. At that time the discussions regards to the relationship between cosmic rays and the earth's geomagnetic field will enter into the new stage impossible to predict.

§ 7. Acknowledgements

The author is indebted to Dr. P. Rothwell of the Depart of Physics, Imperial Institute Road of London, for providing the data in their latitude surveys. He also wishes to express his sincere thanks to Dr. Y. Miyazaki for his constant interest and valuable advise on this study.

References

Compton A.H. and Turner R.N. (1937) Phys. Rev. **52**, 799.
Katz L., Meyer P. and Simpson J.A. (1958) Suppl. Nuovo Cimento **8**, 277.
Kodama M., Kondo I. and Wada M. (1957) J. Sci. Res. Inst. **51**, 138.
Kodama M. and Miyazaki Y. (1957) Rep. Iono. Res. **11**, 99.
Law P.G., Mckenzie C.D. and Rathgeber H.D. (1949) Australian J. Sci. Res. **A2**, 493.
Millikan A. and Neher H. (1936) Phys. Rev. **50**, 15.
Oguti T. and Kodama M. (in press) Nature.
Quenby J.J. and Webber W.R. (1958) Proc. Moscow Meeting.
Rose D. C., Fenton K.B., Katzman J. and Simpson J.A. (1956) Canadian J. Phys. **34**, 968.
Rose D.C. and Katzman J. (1956) Canadian J. Phys. **34**, 1.
Rothwell P. and Quenby J.J. (1957) Proc. Varenna Conference.
Sekido Y., Asano Y. and Masuda T. (1943) Sci. Papers Inst. Phys. Chem. Research **40**, 439.
Simpson L.A., Fenton K.B., Katzman J. and Rose D.C. (1956) Phys. Rev. **102**, 1648.
Storey J.R., Fenton A.G. and McCracken K.G. (1958) Nature **181**, 34.
Wada M. (1957) J. Sci. Res. Inst. **51**, 201.

An Experimental Proof of the Mode Theory of VLF Ionospheric Propagation

By T. Obayashi, S. Fujii and T. Kidokoro

Hiraiso Radio Wave Observatory, Radio Research Laboratories.

(Read October 26, 1958; Received January 10, 1959)

Abstract

A new spectoscope recording continuously the amplitude-frequency spectrum of VLF atmspherics has been developed. The receiver sweeps the frequency giving complete coverage of the band of 5~70 kc/s repeatedly and the output is displayed on an intensity modulated cathode-ray tube, which is photographed on a slowly moving film.

Observations have been carried out and it appears that the result provides an excellent experimental base for the mode theory of VLF ionospheric propagation. It is found that the frequency-spectrum of distant atmospherics shows a broad intensity maximum around 10 kc/s and decreases its intensity towards higher frequencies with undulating peaks. Marked selective absorption bands appeared in the spectrum are variable according to the time of day, and they might be assoiated with cut-off frequencies of the waveguide bounded by the earth and the ionosphere. The solar flare effect on VLF atmospherics propagation is also revealed, which indicates a sudden shift of the spectrum to higher frequencies owing to the increase of ionization and the lowering of a reflecting height of the ionosphere.

1. Introduction

It has been known for many years that atmospherics in the very low frequency band (VLF) can propagate to great distances. In recent years, however, there has been a renewed interest of this problem; many investigators have found an evidence of a pronounced absorption band 2~4 kc/s, while for frequencies around 10 kc/s there is very little attenuation. This has some contradiction to that predicted by the Austin-Cohen law, but in complete accord with the newly developed mode theory of VLF ionospheric propagation. In the mode theory of VLF propagation suggested by Budden (1951), waves that have traveled considerable distances act as if they were propagated in the space between concentric reflecting spherical shells representing the earth and the lower edge of the ionosphere. The observed presence of an absorption band for frequencies of the order of 3 kc/s could be explained as the effect of a cut-off frequency in the waveguide propagation.

In order to elucidate these, Chapman and his colleague (1953, 1956) have made precise observations on wave-form characteristics as well as the amplitude-frequency spectra of individual atmospherics in the audio-frequency band. Results showed that the spectrum of atmospherics varies with the distance of propagation indicating the

existence of an appropriate mode of propagation and of the strong selective attenuation due to ionospheric influences. Further studies both experimental and theoretical sides have been progressed last few years, especially Wait (1957) has made an elaborate computation on the mode theory of VLF ionospheric propagation and showed that the predicted characteristics by the theory well accord with the experimental facts.

In the present investigation, endeavour is made to obtain a more complete experimental proof of the mode theory of VLF ionospheric propagation. A new set of continual recording of amplitude-frequency spectrum of atmospherics is developed. The basic action of this spectroscope is to scan VLF band continuously, the output is displayed on an intensity modulated cathode-ray oscillograph and recorded photographically instead, as conventionally, of recording th amplitudes of signals at several fixed frequencies. The pattern on the photographic film is therefore an intensity modulated plot of frequency against time, and the variations of frequency-spectrum such as the diurnal charcterisitic or ionospheric disturbances are clearly demonstrated.

Thus, it appears that the result should provide an excellent experimental base for the mode theory of VLF ionospheric propagation. The results so far obtained are very encouraging, some new evidences found and their interpretations are also given in the present report.

2. Equipment

The main purpose aimed in the present apparatus is the observation of continual and direct display of the frequency-spectrum of VLF radio waves radiated by atmospherics. Although there are several kinds of spectrum-analyzer which may be applicable for the study of atmospherics, a scanning type of spectroscope is developed by the present requirement of a long continual observation of the frequency-spectrum of atmospherics.

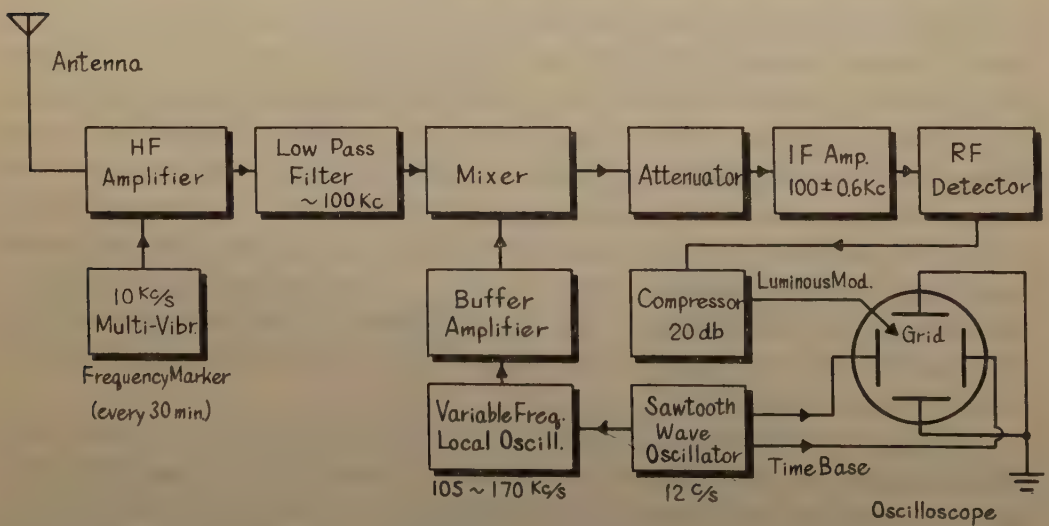

Fig. 1 A block diagram of VLF spectroscope.

The apparatus consists of a set of the conventional VLF atmospherics receiver, a frequency scanning device and a display unit including a phtographic motion camera. A block diagram of this spectroscope is shown in Fig. 1. The antenna is a vertical whip with an effective height of 10 metres. The receiver is superheterodyne type of consisting HF and IF amplifiers, mixer, and detecter, their details are given elsewhere. The local oscillator sweeps frequencies 105~170 kc/s by using a dust-core to alter its inductance, in which the voltage sweep is fed from a sawtooth generator. Simultaneously, a synchronized sweep is applied to the time-base of a cathode-ray oscilloscope, so as a given horizontal position of the oscilloscope spot corresponds uniquely to a single frequency. By mixing this local oscillator with the external signal and applying a narrow band IF transformer of 100 kc/s, the receiving frequency range is converted to the range of 5~70 kc/s. The IF bandwidth is ±600 c/s sufficient enough for the present purpose. The over-all frequency-response of the receiver is shown in Fig. 2. It is evident that the receiver has a flat characteristic over the sweep-frequency range and a sharp cut-off (about –30 db) at the frequencies greater than 100 kc/s.

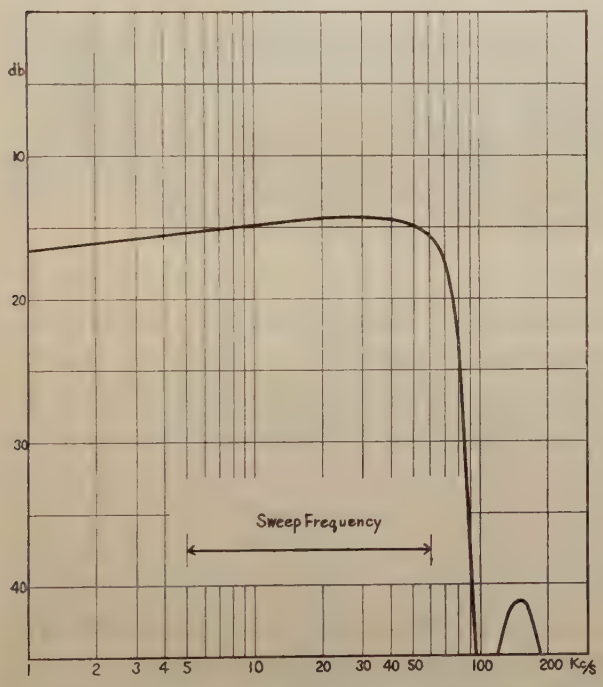

Fig. 2 Frequency-response of the receiver.

Thus, as the receiver sweeps the frequency, giving complete coverage of 5~70 kc/s band, the output is displayed as an intensity modulated line on a cathode-ray oscilloscope. This is photographed on a slowly moving (1.5 cm/hour) 35-mm film, producing a frequency-time record with atmospherics intensity appearing as variations in photographic density. The combination of the film characteristic and the logarithmic compressor permits the recording of a wide range of signal intensities over 20 db in considerable detail. The record is calibrated by the frequency-maker of the 10 kc/s multivibrator every 30 min., which is swiched on automatically by a standard time clock.

This type of VLF atmospherics spectroscope certainly has a major advance over that of recording of atmospherics intensities at a number of single frequencies, and so far the obtained result concerns it has been very succcessful. Since the pattern on the film is an intensity modulated plot, an auxiliary apparatus to reproduce an amplitude-frequency spectrum is also designed. Namely, by successive scanning on the film using a photoelectric tube, an original amplitude of the signal is obtained in db scale with the aid of a suitable comparison technique.

3. Frequency-spectra of atmospherics propagated through the ionosphere

Observation of atmospherics using the present VLF spectroscope has been carried out at the Hiraiso Radio Wave Observatory since June, 1958. Simultaneously the continuous measurment of the intensity of atmospherics at 27 kc/s has also been supplemented. Some of records obtained are reproduced in Pl. 1, which are shown by the

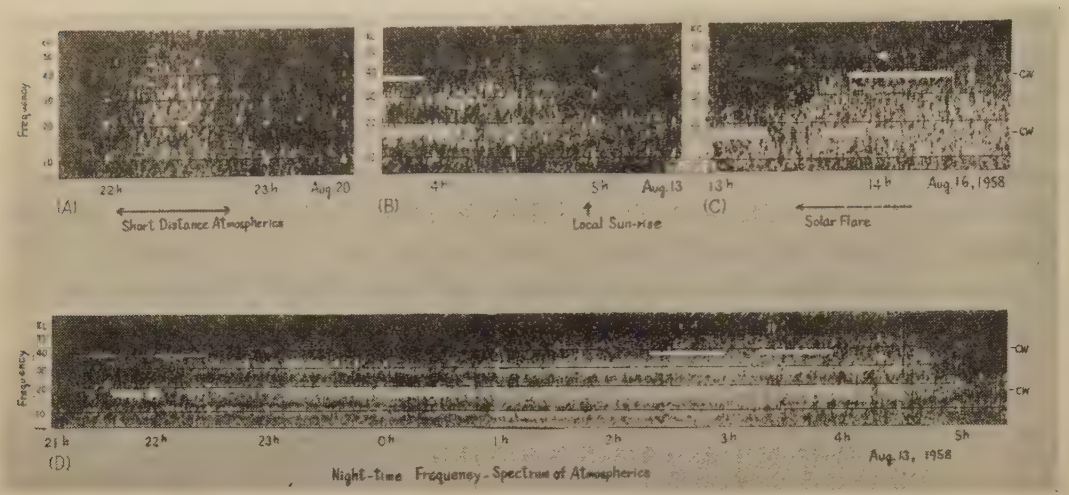

Pl. 1 Frequency-spectra of VLF atmospherics of ionospheric propagation

frequency-vs-local time patterns, highlight and dark portions indicate intense atmospherics and weak or no atmospherics respectively. Signals from radio stations are also recorded, which appear as white straight lines indicated by cw. Frequency-spectra of atmospherics in the VLF band are well represented in these records, however, it must be remarked the following thing to make an exact understanding of these records: Since the duration of atmospherics is usually less than a few millisecond, an individual atmospheric photographed covers only a limited range of the frequency band, owing to the reason that the time-base of the oscilloscope is converted to the frequency-sweep. In other words, the period of sweep-frequency (order of 0.1 sec.) is not long enough to cover the whole spectrum of individual atmospherics. However, if it is assumed that numerous atmospherics are occurring randomly within a short duration and that the original amplitude distribution of atmospherics at the source is statistically homogeneous, the film recorded with a sufficiently long time exposure should reveal the amplitude-frequency spectrum in statistical sense.

Examining through the records, it is found that night-time atmospheics are much intense and extend to the higher frequency than those of day-time. Since there is no such tendency for the short distance atmospherics, the general feature stated above should be restricted for the long distanced atmospherics, which may be largely influenced by the ionospheric condition. It is also noted that the maximum intensity of atmospherics propagated through the ionosphere lies in the frequency range about 10～20 kc/s, as has already been known by studies of wave-forms and field intensity measurements of distant atmospherics.

One of the most outstanding phenomena discovered by the present observation is that there exists certain clear stripe of intensity in frequency which changes regularly with local time, as has been displayed clearly in (B) and (D) of Pl. 1. That is, long distance atmospherics suffer some selective absorption during their propagation through the ionosphere. As shown in (A) of Pl. 1, the short distance atmospherics (probably less than 500 km) do not show such frequency characteristic, therefore absorption bands appeared are certainly due to the effect of ionospheric propagation. Typical amplitude-frequency spectra at night and day-time are shown in Fig. 3, which are obtained with

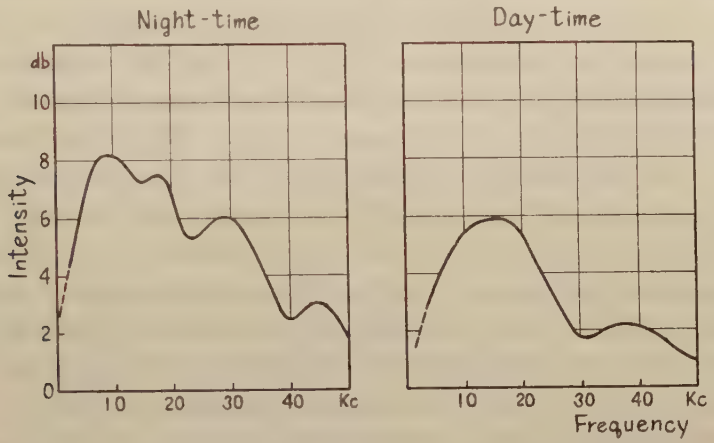

Fig. 3 Typical amplitude-frequency spectra of distant VLF atmospherics. (ordinate: relative intensity in db)

the aid of the photoelectric scanner. The night-time spectrum has its maximum at about 10 kc/s and the intensity decreases towards high frequency with undulating peaks, while the day-time spectrum has smooth double maximums at about 15 kc/s and 40 kc/s, its intensity being weaker than that of night-time. These two types of spectrum interchange rather distinctly at local sun-rise; the night-time pattern is shifted towards higher frequencies as shown in (B) of Pl. 1, though the sun-set transition is less clear as in (D). In Fig. 4, examples of the diurnal variation of amplitude-frequency spectra

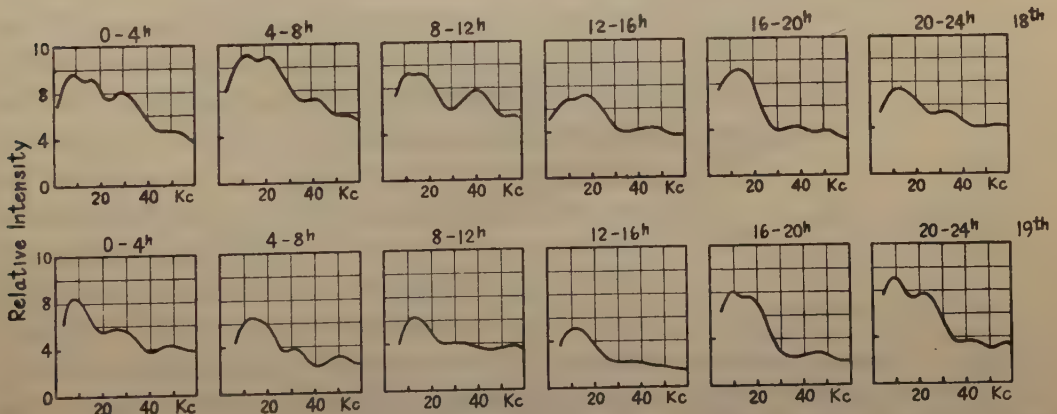

Fig. 4 The diurnal variation of amplitude-frequency spectrum of atmospherics on Aug. 18–19, 1958

are illustrated. Of course, individual frequency-spectra are variable even in the night-time, however, the general tendency mentiond above can be observed considerably well.

This characteristic feature of the amplitude-frequency spectrum of VLF atmospherics can not be explained by the Austin-Cohen law of VLF propagation, but it seems to be likely that the waveguide theory is responsible for this. The conception that VLF radio waves propagate to great distances via multiple reflections in the waveguide bounded by the earth and the ionosphere has been developed by Budden (1951) and Wait (1957) as the mode theory of VLF ionospheric propagation. An essential part of this theory is the existence of definite cut-off frequencies in the modes of waveguide propagation. In order to simplify the evaluation of this mode characteristics, let us consider the ground and the ionosphere to be regarded as a waveguide of perfectly conducting plates. Then, the cut-off wavelengths are given by 2h/n, where n is the integer specifying the number of the mode and h is an effective reflecting height of the ionosphere. When the boundary of the waveguide is not perfectly conducting, as the case of the actual ionosphere, the cut-off wavelength is not sharply defined and the effective reflecting height of the ionosphere would become to be higher.

From the above consideration, the dawn effect of the frequency-spectrum, which is appeared as the shifting of the maximum intensity bands towards higher frequencies, could be explained as the lowering of the ionospheric height or else the increase of the conductivity in the lower ionosphere. On the other hand, it is already known from a number of experiments that the reflecting height varies consistently from 90 km at night to 70 km during the day (Waynick, 1957). Therefore this accords well with the present conclusion.

There is an another interesting fact, lending further support to the mode theory of VLF propagation. That is the effect of SID's, which is known as the sudden enhancement of atmospherics (SEA). An intense solar flare occured at 13*h* 35*m*, Aug. 16, 1958, which was associated with a pronounced SEA in the record of field intensity of atmospherics at 27 kc/s. The record of frequency-spectrum during this period is reproduced in (C) of Pl. 1, and measured amplitude-frequency spectra at pre-flare and during the maximum of the solar flare are also shown in Fig. 5. A sudden shift of the frequency-spectrum at the beginning of the solar flare is evident; the band of strong intensity was around 10~20 kc/s before the flare as in the case of usual day-time, and then at 13 *h* 35 *m* the intensity was raised up, shifting the band of strong intensity towards higher frequencies 15~30 kc/s. Consequently, in the higher frequency band of VLF the intensity of distant atmospherics is enhanced, while at the frequency about 10 kc/s or less a sudden reduction in intensity occurs. This confirms

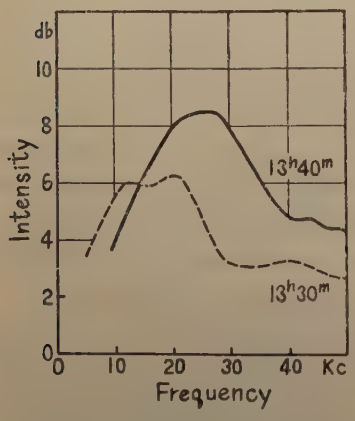

Fig. 5 The frequency-spectrum at the SEA; the dotted line shows the spectrum at pre-flare, and starting time of the solar flare is at 13h 35m (L.M,T.), Aug. 16, 1958.

the result discovered already by Gardner (1950). Since it is known that during SID's the electron density in the lower ionosphere is increased and its height is lowered considerably, these facts would eventually yield the explanation that the reduction of field intensity in the lower VLF band is caused by the shifting the cut-off towards slightly higher frequencies while in the frequencies above the cut-off the intensity is enhanced considerably owing to the good reflection in the lower edge of the ionosphere.

The observed stripe of absorption band is still puzzling. However, it is expected that the actual observed intensity of distant atmospherics must be the sum of contributions from many waveguide modes, which are appreciably influenced by the distance from the source and the condition of the lower ionosphere. A detailed investigation of the theory of the waveguide modes would possibly give the appropriate solution.

In the discussion of the frequency-spectrum of atmospherics, the wave-form characteristics must be mentiond, which has been studied extensively by many researchers in this field. Since the investigation of wave-forms and of frequency-spectrum are merely different approaches to a single phenomenon, their results must be mutually equivalent. Mathematically, the wave-form G(t), the amplitude-frequency spectrum $S(\omega)$ and the phase-frequency spectrum $\phi(\omega)$ have the following mutual relations;

$$G(t)=\frac{1}{\pi}\int_0^{\infty} S(\omega)\cos\left[\omega t+\phi(\omega)\right]d\omega$$

$$S(\omega)=\sqrt{\left[\int_{-\infty}^{+\infty} G(t)\cos\omega t\,dt\right]^2+\left[\int_{-\infty}^{+\infty} G(t)\sin\omega t\,dt\right]^2}$$

and

$$\phi(\omega)=\tan^{-1}\left[-\int_{-\infty}^{+\infty} G(s)\sin\omega t\,dt \;\Big/\; \int_{-\infty}^{+\infty} G(t)\cos\omega t\,dt\right].$$

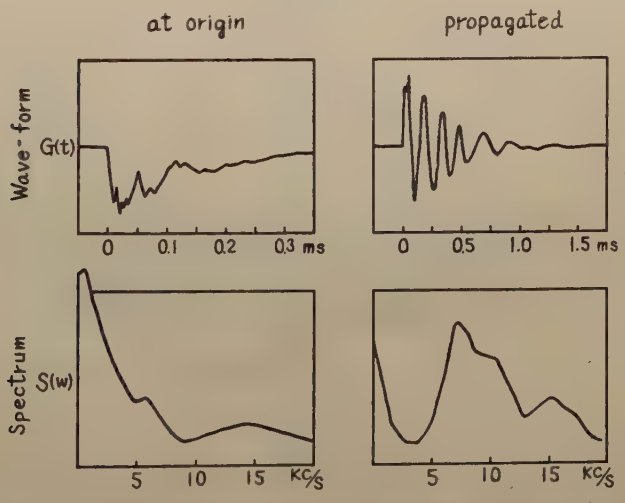

Fig. 6 The wave-forms and corresponding amplitude-frequency spectra for atmospherics at the origin and that of propagated through the ionosphere. (after Kazuo Sao)

Therefore, from the known wave-form it is possible to compute its frequency-spectrum. Using an analog computer of this Fourier transform expressions, Sao (1958) has made the frequency analyses of a number of wave-forms of atmospherics. Two type of frequency-spectrum are characteristic, one is of the origin of an atmospheric and the other is of a distant atmospheric. Those wave-forms and their spectra obtained by him are reproduced in Fig. 6. The frequency-spectrum at the origin of a lightning stroke shows a remarkable decrease of amplitude towards higher frequencies, having almost flat characteristics at about 10~30 kc/s. This result accords with the frequency-spectrum of short distance atmospherics shown in (A) of Pl. 1. Wave-forms at distant atmospherics are more complicated and show the influences of the ionosphere. The obtained spectrum indicates heavy attenuation around 2~5 kc/s and less attenuation at the lower frequency end and at around 10 kc/s, which is generally in good agreement with our observations.

An another investigation has been carried out by Champan and Matthews (1953), who used a spectroscope of a number of narrow band-pass filters tuned to frequencies in the range of 40 c/s to 16 kc/s, recording the amplitude-frequency spectra and corresponding wave-forms for individual atmospherics. They also discussed the relation between the wave-form characteristics and the significant changes in the spectrum as the distance of propagation increases. Summing up their results, Chapman and Macario (1956) derived attenuation curves with respect to frequency for those of distant atmospherics. It is indicated that in the frequency range from 200 c/s~10 kc/s the greatest increase of attenuation occurs at about 2 kc/s, it being about 20 db per 1000 km by day and 10 db by night.

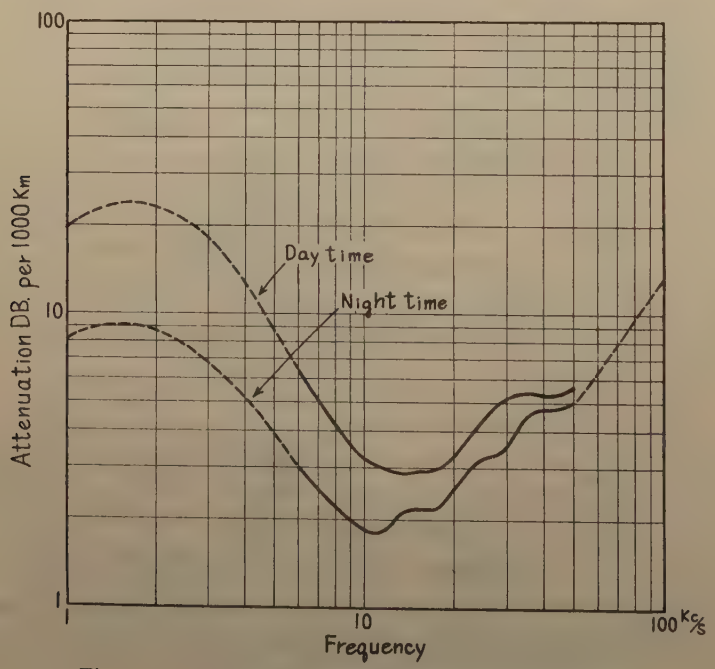

Fig. 7 The variation of attenuation with frequency.

Here, it might be worthwhile to link up this with our result. For this purpose, the frequency-spectra shown in Fig. 3 can be used. Since their curves were given by attenuation in db per 1000 km, our result must have to convert into this scale. Although the distribution of atmospherics source originating can not be identified in the present observation, according to Kimpara and Kimura (1958) distant atmospherics received in Japan mainly come from the sources in the south-west direction during summer night, viz. from regions south and east China and Phillipines. Therefore the average distance from the sources is of the order of 2000 km. Assuming this and also that the minimum attenuation around 10 kc/s is about 2~3 db per 1000 km, the variation curve of attenuation with frequencies of 1~100 kc/s is illustrated in Fig. 7. The curve for the frequency range of 1~10 kc/s is taken from Chapman and Macario's, and for 50~100 kc/s is used Eckersley's values (1932). This curve gives a general idea which VLF waves are attenuated and can propagate to great distances.

Conclusion

The continual observation of the frequency-spectrum of atmospherics reveales important characteristics of VLF radio waves propagated through the ionosphere. The general agreement between the experimental and theoretical results both substantiates the mode theory and the experimental method followed in this work. The fact that certain bands of VLF radio waves propagate to great distances with small attenuation should be useful for long range navigational systems, world-wide communications or standard radio wave systems, and tracking of atmospheric storms.

A further investigation is undertaken and two sets of spectroscope covering the frequency bands of 200 c/s~10 kc/s and 10~100 kc/s are now in operation, which will make a comlete coverage of major frequency-spectrum of atmospherics.

References

Budden K.G. (1951) Phil. Mag. **42**, 1.
Chapman F.W. and Matthews W.D. (1953) Nature **172**, 495.
Chapman F.W. and Macario R.C.V. (1956) Nature **177**, 930.
Eckersley T.L. (1932) J. Inst Elect. Eng. **71**, 405.
Gardner F.F. (1950) Phil. Mag. **41**, 1259.
Kimpara A. and Kimura Y. (1958) Proc. Res. Inst. Atmospherics, Nagoya Univ. **5**, 21.
Sao K. (1958) Proc. Res. Inst. Atmospherics, Nagoya Univ. **5**, 12.
Wait J.R. (1957) Proc. Inst. Radio Eng. **45**, 760.
Wait J.R. (1957) Proc. Inst. Radio Eng. **45**, 768.
Waynick A.H. (1957) Proc. Inst. Radio Eng. **45**, 741.

The Absolute Measurement of the Concentrations of the Radioactive Substances in the Atmosphere, in Tokyo

By M. KAWANO

Electrotechnical Laboratory, Tokyo.

S. NAKATANI

Tokyo College of Science, Tokyo.

(Read May 17, 1958; Received February 18, 1959)

Abstract

Comparing with the already known concentration of radon emanated from the radium standard solution, the absolute measurement of the concentrations of the radioactive substances in the atmosphere was carried out by the ionization chamber method. The concentrations of the radioactive substances in the atmosphere were $2.3 \sim 12.0 \times 10^{-16} C/cm^3$ on fine days.

The ratio of the ionization current by beta-, gamm-raditions to that by total radiations in the air of definite volume is about 5～25 percent, and is very larger than that in radon being in the state of radioactive equilibrium with its decay products (the ratio is about 2～3 percent).

1. Introduction

The concentration of the radioactive substances in the atmosphere is very important from the view point of atmospheric physics and health physics. The presence of the radioactive substances influences the rate of ion pair production in the atmosphere and the ionization equilibrium state. And also, their presence influences the lung dose of human.

The measurements of the concentration of the decay product of radon in the atmosphere have been carried out by the several authors (Aliverti;, 1932; Garrigue, 1951; Harley, 1953; Wilkening, 1956; Blifford et al., 1952) at many places in the world. These authors measured by the indirect methods which require the assumption that radioactive equilibrium comes into existence at all times between radon and its decay products. In the case of researching the time variations of the concentrations of the radioactive substances in the atmosphere, the results obtained by the indirect method seem to be almost correct. Because, the concentrations of the substances collected by the several collection methods seem to be almost proportional to the total concentrations of the substances. But, the direct methods must be used for obtaining the accurate values. Hess and Vancour (1950), Hess (1953) and Cotton (1955) have been measured the rate of ion pair production by each ionizing agent with ionization chambers. But, the results of their measurements did not give directly the concentrations of the radioactive substances in the atmosphere. Miranda (1957) measured the concentration of radon by

the charcoal trap method, and measured (Miranda, 1958) the rate of ion pair production by beta-radiation in the atmosphere by ionization chambers. The charcoal trap method seems to be very excellent for the measurement of the concentration of radon. But, this method is not suitable for the continuous measurement.

To discuss the problem of the radioactivity in the atmosphere, it is very important to clarify that the radioactive equilibrium between radon and its decay products in the atmosphere comes into existence or not. In this paper, the results of absolute measurements of the concentrations of the radioactive substances in the atmosphere is reported. In the case of measureing the concentrations of the radioactive substances in the atmosphere, it is necessary to ascertain the radioactive equilibrium between radon and its decay products. From this point of view, the ratio of the ionization current by alpha-ray contained in air of definite volume to that by beta-, gamma-rays is measured.

2. Instruments

The instruments used for this measurement are the two ionization chambers of different thickness. And, each chamber is held in the cylindrical case of iron plate of 3 mm thickness. The centre of chamber coincides with that of iron case. As the iron case is air-tight, that is able to be evacuated. The ionization chamber used for the measurement of the ionization current by alpha-, beta-, gamma-rays shown in Fig. 1. The chamber is constructed of wire mesh cylinder, with dimensions of 1 cm in diameter and 40 cm long, having a volume of 3,150 cm^3, which is also covered with wire mesh. The screen are composed of 0.3 cm mesh. The inner screen is maintained at −1,300 volts. The distance between the outer screen and the outer one is about 5 mm, and the inner screen is insulated from the outer one. The electric field intensity is sufficient to capture the ions contained in the air flown into the ionization chamber from the outside. A 1,300 volts battery provided the sweep voltage for alpha chamber. About 300 volts is found to be sufficient for saturation current of this chamber in the case of alpha-ray; but, 1,300 volts is necessary to capture perfectly the ions contained in the air flown into the ionization chamber from the outside. The inner electrode of chamber is consisted of a brass rod about 5 mm in diameter, and protruded through an teflon plug which is mounted in a suitable guard-ring arrangement. To minimize influence of the water vapour contained in the air flown into the chamber, the special device is given for the protection of the insulator. The electrodes of the chambers are connected to the vibrating reed electrometer (Appl. Phys. Co., U.S.A.) respectively, and the measuring values are self-recorded by the automatic

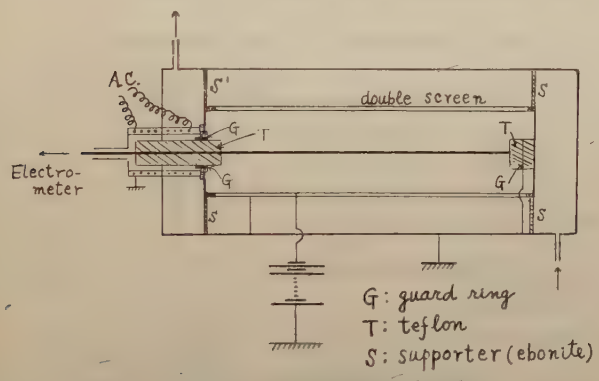

Fig. 1 The screen ionization chamber.

balancing self-recording ammeter (Yokogawa Electric Works, Co., Japan). Comparing the ionization current by the examining air with that by radon of already known concentration, the absolute values of concentrations of the radioactive substances are obtained.

The ionization chamber used for the measurement of the ionization current by beta-, gamma- radiations in the atmosphere is the same as the one used for the measurement of the total radiations excepting the side wall. The side wall of the beta-, gamma- chamber is aluminium of 40 micron thick (11mg/cm^2). And, 90 volts battery provided the sweep voltage for beta-, gamma- chamber. This voltage is sufficient for saturation current of this chamber.

3. Calibration

The radon gas emanated from the radium standard solution of already known concentration was used for the calibration of the concentration of the radioactive substances in the air. The radon emanated from the radium standard solution is drawn into the ionization chamber which is previously evacuated. Radon free air was forced through the solution (contained in a standard 500 cc de-emanating flask) at the rate of 2l/min. As clarified by Miranda (1958), the radioactivity of different portions of bubbling gas during de-emanation is remarkably different. In the case of our experiments, the activity of different portions of bubbling gas during de-emanation are shown in Table 1.

Table 1 Radioactivity of different portions of bubbling gas during de-emanation.

Amount of bubbling gas discarded previous to passing into ionization chamber (litres)	Portion of bubbling gas passed into ionization chamber	Activity at time of de-emanation (arbitrary unit)
0	1st	26
15.7	2nd	5
31.4	3rd	3
47.1	4th	2

In this experiment, the first portion of bubbling gas during de-emanation was used for calibration in each case.

The charcoal trap consisted of about 200 gr of cocoanut charcaoal in granular form confined within a tube as shown in Fig. 2. The trapping efficiency of charcoal for radon gas was researched by Miranda, and may be sufficient for obtaining the radon free air. Then, the air passed through the charcoal trap seems to be free from radon. The trapping efficiency of charcoal for the radioactive dust (carriers of RaA, RaB and RaC) is measured by the electrostatic precipitator and G-M counter (Kawano and Nakatani, 1959). Then, it is found that the radioactive dust is almost trapped by charcoal, and the air passed through the charcoal trap seems to be free from the radioactive dust. According to the results of these measurement, the charcoal trap may be used for obtaining the radioactive free air. Then, the charcoal trap is used for obtaining the zero value of ionization current in

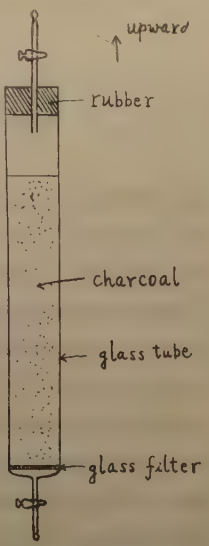

Fig. 2 The charcoal trap tube.

this measurement.

Fig. 3 shows the relation between the concentration of radon in the ionization chamber (screen) and the ionization current. The concentration of radon is obtained under the condition of the radioactive equilibrium between radon and its decay products.

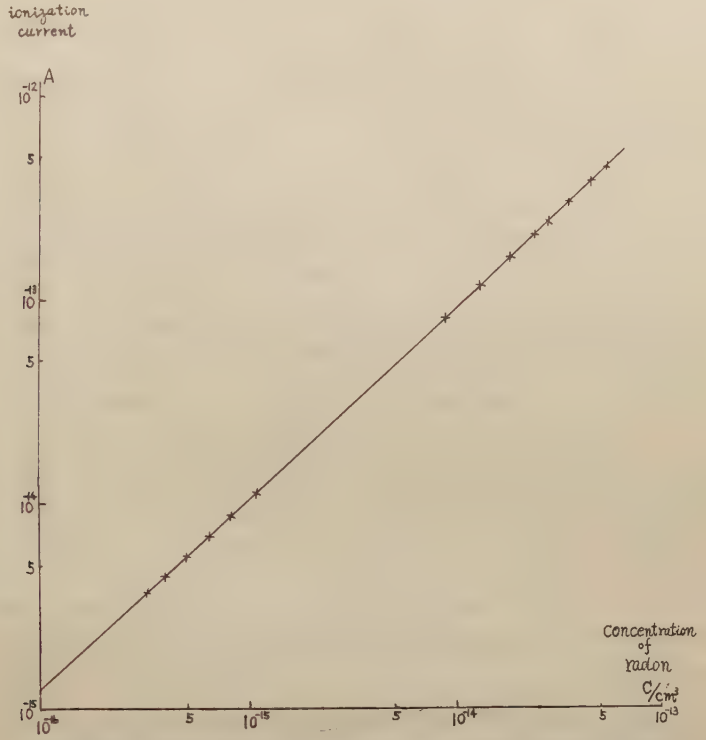

Fig. 3 The relation between the concentration of radon and the ionization current by total radiations

4. Measurement

Fig. 4 shows the arrangement used for measurement of the concentrations of the radioactive substances in the atmosphere. A is the ionization chamber (screen), and B is the ionization chamber (aluminium foil). C, D are the vibrating reed electrometers, and E is the self-recording ammeter. F is the suction pump (13 l/m) used for drawing the air of out door through a vynil pipe.

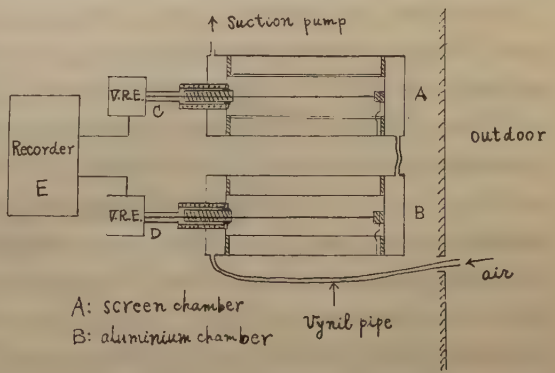

Fig. 4 The distribution of instruments used for measurement of ionization current.

Fig. 5 shows the time variation of ionization current by total radiations in the air of definite volume. The concentrations of the radioactive substances are obtained from the relation between the ionization current and the con-

centration of radon (equilibrium with its decay products) shown in Fig. 3. Table 2

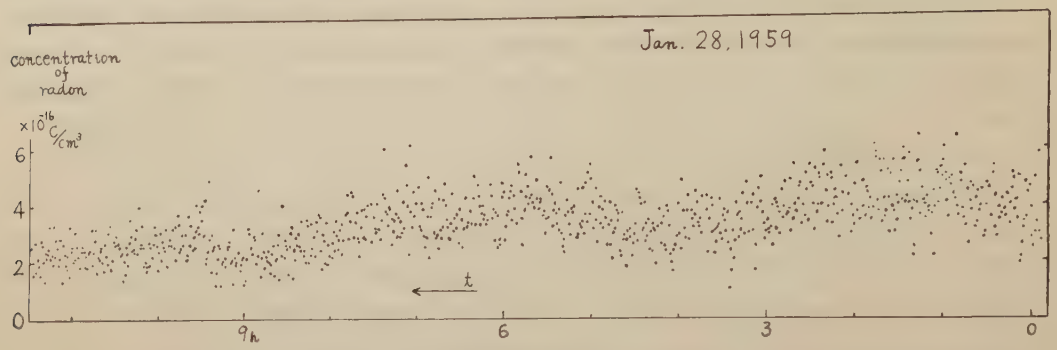

Fig. 5 An example of the record of the time variation of ionization current by total radiations in the atmosphere.

Table 2 The measured values of the concentration of the radioactive substances in the atmosphere on fine days. (Nov. 1958～Feb. 1959)

	daytime ($\times 10^{-16}$C/cm^3)		night ($\times 10^{-16}$C/cm^3)	
	max. value	min. value	max. value	min. value
limited values	12.0	2.3	11.0	4.2
mean values	5.5		7.0	

shows a summary of results obtained from Nov. 1958 to Feb. 1959. The single remarkable feature of all measurement was the wide fluctuations from day to day, and from time to time.

The variations of concentration of radioactive substances on rainy days are very complicated, as described in the previous paper (Kawano and Nakatani, 1958) about the rate of ion pair production. The origins of this complicated variations seem to be connected directly to the change of radon exhalation from the underground during the rainfall. But, the detailed discussion on the variation under the rainy condition must wait the further investigations.

The ratio of ionization current by total radiations to that by beta-, gamma- radiations. Under the condition of the radioactive equibrium between radon and its decay products, the ratio of the ionization current by alpha radiation to that beta-, gamma-radiations contained in the air of the definite volume was measured by the ionization chambers shown in Fig. 4. In this case, the factor which affects the ratio of the ionization current measured by each chamber is absorption of beta-radiation by aluminium foil. Assuming the mean energy of the beta-radiation from RaB and RaC being 0.5MeV, it can be easily computed that this effect contributes about 5 per cent to the measured ionization current. Therefore, in order to correct this effect, the measured values of ionization current by beta-, gamma- radiations must be divided by 0.95.

At first, the two ionization chambers were evacuated, and filled up by air passed through the standard radium solution in flask.

At the time of three hours after filling up, the radioactive equilibrium between radon and its decay products comes into existence. This process is shown by the growth curve of ionization current. The relation between the concentration of radon and the ionization current by total radiations is shown in Fig. 3. The relation between the concentration of radon and the ionization current by beta-, gamma- radiations is shown in Fig. 6. Comparing the relation between the concentration of radon and the ionization

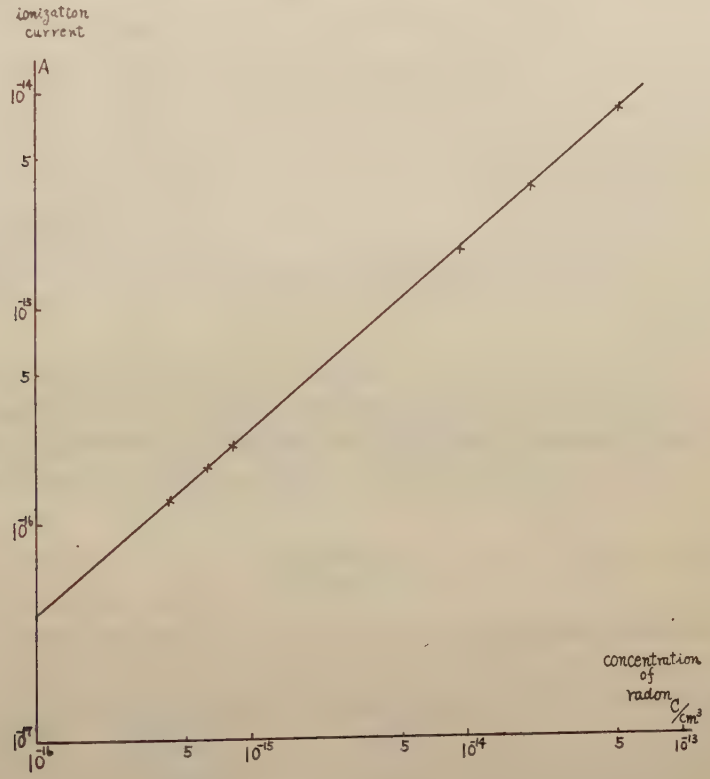

Fig. 6 The relation between the concentration of radon and the ionization current by beta-, gamma-radiations (build up method).

current by beta-, gamma- radiations shown in Fig. 6 with that shown in Fig. 3, the ratio of the ionization current by beta-, gamma- radiations to that by total radiations was obtained. The ratio is 2～3 per cent. The air is drawn through the two ionization chambers by suction pump. Fig. 7 shows a few examples of time variations of the ionization current by total radiations and beta-, gamma- radiations in air of outdoor of definite volume. As shown in this figure, the values of ionization current by beta-, gamma- radiations fluctuated considerably from hour to hour. Table 3 shows a few examples of the hourly mean values of the ionization current by beta-, gamma- radiations and total radiations.

As shown in this table, the ratio of the ionization currents by beta-, gamma-radiations to that by total radiations is 5～25 percent.

Generally speaking, the ratio is small at night and on rainy day, and large in the daytime. The ionization current by each chamber was also measured by the build up

method, and the results were coincident with those shown in Table 3.

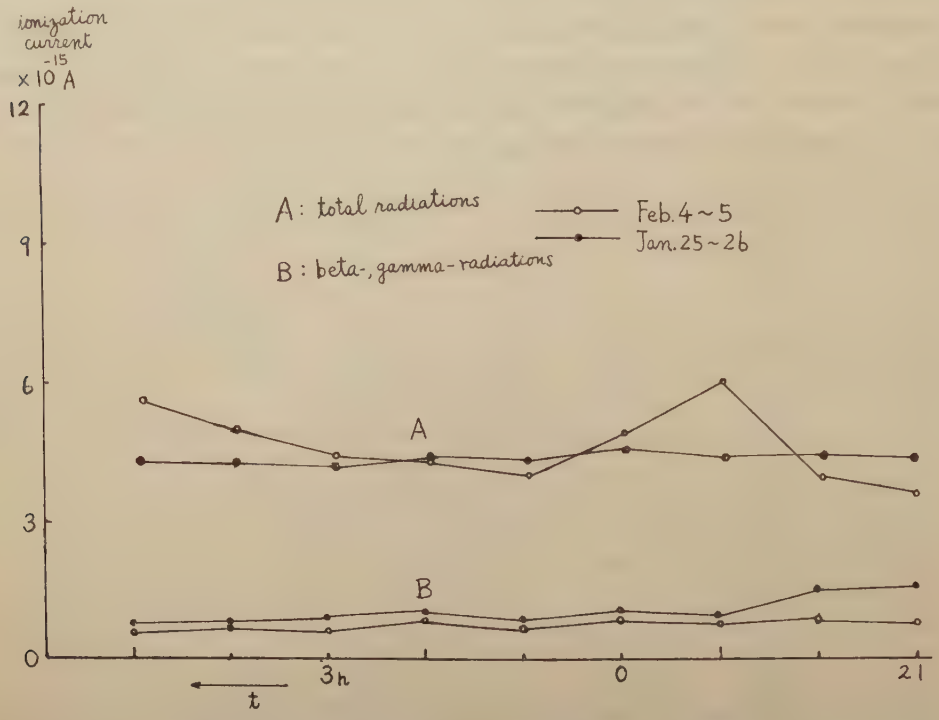

Fig. 7 A few examples of time variations of ionization current by radioactive substances in the atmosphere.

Table 3 A few examples of the ionization current by radioactive substances in the atmosphere.

ionization current / date	(I) ionization current by total radiations	(II) ionization current by beta-, gamma-radiations	ratio (II)/(I) %
Jan. 28, 1959	2.0×10^{-15}A	0.5×10^{-15}A	25.0
,,	3.5×10^{-15}A	0.5×10^{-15}A	14.2
Feb. 5, 1959	10.5×10^{-15}A	0.6×10^{-15}A	5.8
,,	4.5×10^{-15}A	0.5×10^{-15}A	11.0

6. **Discussion of results.**

As previously described, the ionization current due to beta-, gamma- radiations is about 2~3 per cent of that by total radiations under the condition of radioactive equilibrium between radon and its decay products. The ionization current by beta-, gamma radiations is 5~25 per cent of that by total radiations in air of definite volume. The discrepancy of these two cases seems to show that radon is not in the state of radioactive equilibrium with its decay products. This fact is very important for obtaining the concentration of the radioactive substances in the atmosphere. But, there is not suitable method for obtaing the concentration of the radioactive substances in the air under the condition of not radioactive equilibrium. The preparation of this research is now progressing by authors.

7. Conclusion

The concentrations of radioactive substances in the atmosphere were measured by the ionization chamber method continuously. To obtain the absolute values, the concentrations measured by the ionization chamber were compared with those of radon deemanated from the radium standard solution. The values of the radioactive substances in the atmosphere, in Tokyo, is $2.3 \sim 12 \times 10^{-16} C/cm^3$. To clarify the state of the radioactive equilibrium in the atmosphere, the ratio of the ionization current by beta-, gamma-radiations to that by total radiations in the air of definite volume was measured, and the ratio of $(\beta, \gamma)/(\alpha, \beta, \gamma)$ is found to be equal to 5～25 per cent. This ratio was compared with that in radon being equilibrium with the decay products. The ratio in radon was 2～3 percent. The discrepancy seems to show that radon in the atmosphere is not equilibrium with its decay products.

To obtain the concentration of the radioactive substances in the atmosphere, it is important to take into consideration that radon is not equilibrium with its decay products.

In concluding, the authors wish to express their sincere thanks for Dr. T. Hamada, Research Institue of Physics and Chemistry, for his kind arrangement of the standard radium solution. And also, they indebted to Dr. T. Doke, St' Paul University, for his kind discussion on this work.

References

Aliverti G. (1932) Nuovo Cim. **9**, 313.
Blifford I.H.Jr., Lockhart L.B. and Rosenstock H.B. (1952) N.R.L. Report 4036, Sept.
Cotton E.S. (1955) J.A.T.P. **7**, 90.
Garrigue H. (1951) Comp. Reng. Acad. Sci., Paris **232**, 722.
Harley J.H. (1953) Nuclenoics **11**, 12.
Hess V.F. (1953) J.A.T.P. **3**, 172.
Hess V.F. and Vancour (1950) J.A.T.P. **1**, 13.
Kawano M. and Nakatani S. (1958) Journ. Meteor. Soc. Japan **36**, 13.
Kawano M. and Nakatani S. : being published in near future.
Miranda H.A. (1957) J.A.T.P. **11**, 272.
Miranda H.A. (1958) J.G.R. **63**, 147.
Miranda H.A. (1958) J.A.T.P. **12**, 81.
Wilkening M.H. (1956) Trans. Amer. Geophys. Union **319**, 177.

LETTERS TO THE EDITORS

Latitude Variation of Cosmic Ray Intensity Decreases at Sea-Level*

(Received November 18, 1958)

In a recent communication (Brown, 1958) to this Journal, the results of calculations on the influence of modulation effects on the solar flare radiation of February 23, 1956 were reported. In this problem, the flare radiation coming from the sun was considered to be modulated| downward by a geocentric mechanism, the modulation function describing these effects having the from

$$(M)N=\frac{N^{3/2}}{N^{3/2}+K}$$

where N is the magnetic rigidity of the primary radiation and K is a constant. This function was based on an analysis of the nucleonic intensity decreases at mountain altitudes for the period surrounding the flare event; sea-level observations were not considered since a yield function applicable at this altitude had not been determined at that time. The results of the calculations indicated that the effects of modulation on the flare radiation was to flatten the rigidity spectrum, the exponent of the "effective spectrum" observed at the earth being approximately 10% less than that for flare radiation prior to modulation.

Since the latitude effect for the nucleonic component of cosmic radiation at sea-level (Simpson, Fenton, Katzmann and Rose, 1956) and mountain altitudes (Simpson and Fagot, 1956) differ appreciably, it is of interest to extend these modulation calculations to lower altitudes and to determine to what extent the latitude variation of intensity decreases at sea-level agree with predictions based on the modulation function obtained from mountain altitude observations. In order to carry out the sea-level calculations, it was necessary to fit the sea-level latitude curve (Simpson, Fenton, Katzmann and Rose, 1956) with a yield function of the form

$$S(E_0\ 1030)=C\left(\frac{E}{E+E_0}\right)^3 \ln\left(\frac{1+E}{1+E_0}\right)$$

where $E_0=1.18$ Bev/nucleon. Following the procedure used in the mountain altitude calculation (Brown, 1958), this yield function was combined with the modulation function and primary spectra to obtain the latitude variation of intensity decreases at sea-level; the results of these calculations are shown by the dashed curve in Fig. 1 (the solid curve refers to the variations at mountain altitudes, derived previously). Except for the observations from Berkeley, the sea-level curve is seen to be in reasonable agreement

* Supported in part by the joint program of the U. S. Office of Naval Research and the U. S. Atomic Energy Commission. Reproduction in whole or in part is permitted for any purpose of the United States Government.

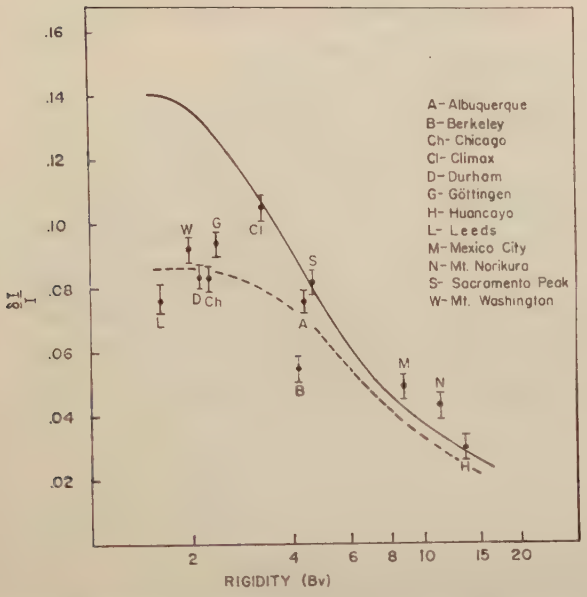

Fig. 1 Latitude Variation for the Intensity Decrease in February 1956 (solid linemountain altitudes; dashed line-sealevel).

with the experimental data. The fact that the Berkeley observations fall below the curve probably results from the location of the monitor under approximately 180 gm/cm^2 of concrete during February 1956. It is also evident from Fig. 1 that the intensity variation observed at Mt. Washington (820 gm/cm^2 atmospheric depth) is only slightly larger than sea-level observations obtained with monitors situated at nearby latitudes. However, the Mt. Washington observations should not be compared with the sea-level variations but with others at a comparable altitude for which the latitude curve for intensity decreases lies approximately halfway between the two curves in Fig. 1.

The difference between the latitude curves for neutron monitors at sea-level and mountain altitudes not only has the effect of reducing the magnitude of nucleonic intensity variations at low altitudes below those at mountain altitudes, but also levels off the amplitude of the low altitude intensity variations at a slightly lower magnetic rigidity than at mountain altitudes. Since separate yield functions are required in these calculations, it is important to make comparisons only between observations obtained at comparable atmospheric depths; this is particulary true at high latitudes, as seen in Fig. 1. In addition, these consideaations indicate the necessity of establishing sea-level neutron monitors at low and equatorial latitudes so as to provide a complete network of monitors at one depth in the atmosphere.

Acknowledgment

The author wishes to express his appreciation to Mrs. Helen G. Hartmann for her assistance with the numerical calculations.

References

Brown R.R. (1958) J. Geomag. Geoelec. **10**, 1.

Simpson J.A. and Fagot W.C. (1956) Phys. Rev. **90**, 1068.

Simpson J.A., Fenton K.B., Katzmann J. and Rose D.C. (1956) Phys. Rev. **102**, 1648.

By Robert R. Brown

Department of Physics,
University of California, Berkeley, California

On the Geomagnetic *Sd* Field

(Received February 5, 1959)

The origin of the disturbance daily variation *SD* of geomagnetism is not yet clear. In 1945, Wulf suggested a possibility that all geomagnetic variations, except secular changes, are due to winds in the upper atmosphere, and later some workers (Rikitake, 1948; Fukushima, 1953; Matsushita, 1953; Vestine, 1954; Jacobs and Obayashi, 1957) attempted to interpret geomagnetic disturbances by the dynamo theory. It seems, however, impossible (for two-dimensional case) to interpret the *SD*-field by the dynamo

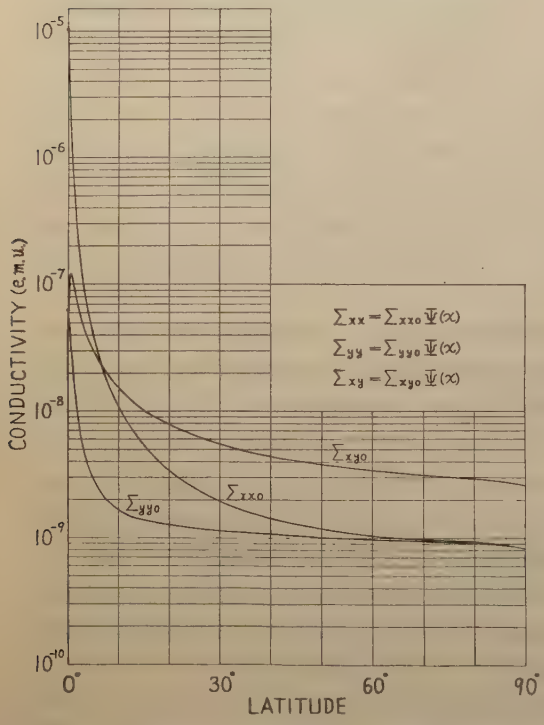

Fig. 1. Latitude distribution of height-integrated conductivities Σ_{xx0}, Σ_{yy0}, and Σ_{xy0}

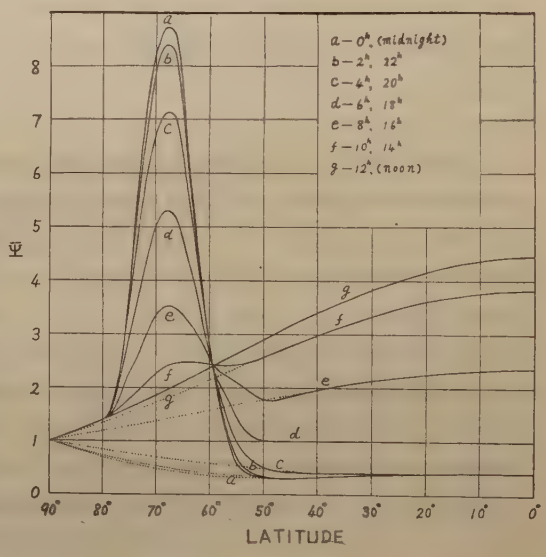

Fig. 2. Latitude distribution of $\Psi(\varphi, t)$ at intervals of two-hours, where the full lines show the value on disturbed days, and the dotted lines show that on quiet days.

theory, unless an exceptionally enhanced conductivity or a very strong wind system (Maeda, 1957) in the polar regions is assumed. In this report we discuss the electric field necessary to produce average disturbed-day daily magnetic variation $Sd(=Sq+SD)$, based on data during the Second Polar Year.

If we suppose that *Sd* is due to the electric current flowing in the *E*-region of the ionosphere as well as *Sq*, the horizontal component $\Delta \boldsymbol{H}_d$ is expressed as follows:

$$\Delta \boldsymbol{H}_d \propto \boldsymbol{I}_d = [K_d](\boldsymbol{E}_d + \boldsymbol{V}_d \wedge \boldsymbol{H}), \qquad (1)$$

where $[K_d]$ indicates the conductivity tensor, and $\boldsymbol{H}$ is the geomagnetic field. In the ordinary dynamo theory, $\boldsymbol{E}_d$ in (1) means the polarization (or electrostatic) field due to the current induced by winds $\boldsymbol{V}_d$. As mentioned above, however, it seems difficult to explain observed $\Delta\boldsymbol{H}_d$ by using accepted values of conductivity K_d and wind velocity $\boldsymbol{V}_d$. Hence, it will be needed to reexamine the expession (1).

From the observed results of ionospheric drift in the E-region, it would be reasonable to assume that the wind velocity on disturbed days is equal to that on quiet days. Then (1) may be rewritten as

$$\Delta\boldsymbol{H}_d \propto \boldsymbol{I}_d = [K_d](\boldsymbol{E}_d' + \boldsymbol{V}_q \wedge \boldsymbol{H}). \qquad (2)$$

$\boldsymbol{E}_d'$ in (2) bears no longer the same meaning as $\boldsymbol{E}_d$ in (1), so we put

$$\boldsymbol{E}_d' = \boldsymbol{E}_d^i + \boldsymbol{E}_d^e, \qquad (3)$$

where $\boldsymbol{E}_d^i$ denotes the polarization field due to the current induced by $\boldsymbol{V}_q$, and $\boldsymbol{E}_d^e$ denotes a polarization field applied probably from the external. $\boldsymbol{E}_d'$ in (2) could be estimated from the observed geomagnetic variations $\Delta\boldsymbol{H}_d$ if K_d and $\boldsymbol{V}_q$ are known. For an example, if we take K_d as shown in Figs. 1 and 2, and $\boldsymbol{V}_q$ as deduced in our previous paper (Maeda, 1955), then $\boldsymbol{E}_d'$ is obtained as shown in Fig. 3. Fig. 4 shows,

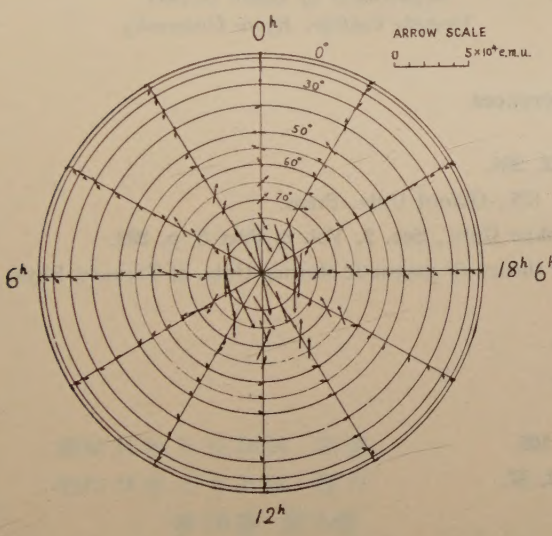

Fig. 3. The polarization fields $\boldsymbol{E}_d'$ on disturbed days, viewed from above the north pole.

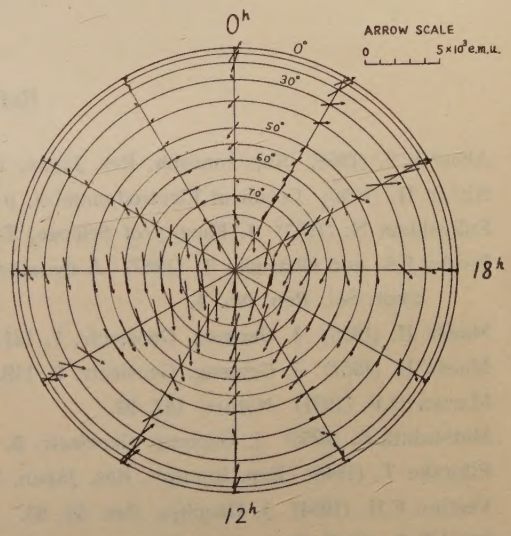

Fig. 4. The polarization fields $\boldsymbol{E}_q$ on quiet days, viewed from above the north pole.

for comparison, the polarization field $\boldsymbol{E}_q$ deduced from the dynamo theory of S_q (Maeda, 1955). It seems from Fig. 3 that $\boldsymbol{E}_d'$ consists of a strong polar field (about 5×10^4 e. m. u.) directed from midnight to noon and a somewhat complicated weak interzonal field.

It is difficult, in general, to obtain separately $\boldsymbol{E}_d^i$ and $\boldsymbol{E}_d^e$ from $\boldsymbol{E}_d'$. However, if we suppose, e.g., as suggested by Alfvén (1950), that the ionospheric current due to $\boldsymbol{E}_d^e$ flows so as to complete its circuit along the lines of magnetic force, through an equatorial current ring, it may be possible to estimate approximately $\boldsymbol{E}_d^i$ and therefore $\boldsymbol{E}_d^e$.

In this case, since there are no sources or sinks of the current due to $\boldsymbol{E}_d^i + \boldsymbol{V}_q \wedge \boldsymbol{H}$, we can put

$$div\left\{[K_d](\boldsymbol{E}_d^i + \boldsymbol{V}_q \wedge \boldsymbol{H})\right\} = 0, \qquad (4)$$

where *div* should be taken on a thin spherical shell (ionosphere) as a currene layer. As it requires great efforts to solve this equation for $\boldsymbol{E}_d^i$, without using Electronic Computer, this result will be reported later. But it may be expected that in the polar regions $\boldsymbol{E}_d^e$ is fairly greater than $\boldsymbol{E}_d^i$, because the order of magnitude of $\boldsymbol{E}_d^i$ inferred from $\boldsymbol{E}_q$ is 1×10^4 e. m. u. at the most.

The cause of $\boldsymbol{E}_d^e$ is not yet certain. Although some workers (Alfvén, 1950; Martyn, 1951; Akasofu, 1958) proposed interesting ideas for the production mechanism of strong polar electric field during magnetic disturbances, in order to explain observed facts, further study will be needed.

I am much indebted to Dr. Y. Inoue, of Technical Research Institute, National Defence Agency, Tokyo, for his helpful discussions.

By Hiroshi MAEDA
Department of Earth Science
Yoshida College, Kyoto University

References

Akasofu S. (1958) Rep. Ionosph. Res. Japan, **12**, 268.
Alfvén H. (1950) Cosmical Electrodynamics, p. 175; Oxford Univ. Press.
Fukushima N. (1953) J. Faculty of Science, Tokyo Univ., Sec. 2, Vol. 8, Part 5, p. 293.
Jacobs J.A. and Obayashi T. (1957) A dynamo theory of magnetic storms, Univ. of Toronto, Phys. Dept. Sci. Rep. No. 4.
Maeda H. (1955) J. Geomag. Geoelectr. **7**, 121.
Maeda H. (1957) J. Geomag. Geoelectr. **9**, 119.
Martyn D.F. (1951) Nature, **167**, 92.
Matsushita S. (1953) J. Geomag. Geoelectr. **5**, 109.
Rikitake T. (1948) Rep. Ionosph. Res. Japan, **2**, 57.
Vestine E.H. (1954) J. Geophys. Res. **59**, 93.
Wulf O.R. (1945) Terr. Mag. **50**, 185 and 259.

昭和34年2月28日　印刷
昭和34年3月5日　發行
第10巻　第2號

編輯兼發行者　日本地球電氣磁氣學會
代表者　長谷川万吉

印刷者　京都市南区上鳥羽唐戸町63
田中幾治郎

賣捌所　丸善株式會社京都支店
丸善株式會社 東京・大阪・名古屋・仙台・福岡

JOURNAL OF GEOMAGNETISM AND GEOELECTRICITY

Vol. X No. 2

1 9 5 9

CONTENTS

World-Wide Distribution of Cosmic-Ray Neutron Intensity at Sea Level ..... M. KODAMA 37

An Experimental Proof of the Mode Theory of VLF Ionospheric Propagation .. T. OBAYASHI, S. FUJII and T. KIDOKORO 47

The Absolute Measurement of the Concentrations of the Radioactive Substances in the Atmosphere, in Tokyo....M. KAWANO 56

LETTERS TO THE EDITORS:

Latitude Variation of Cosmic Ray Intensity Decreases at Sea-Level ..... R.R. BROWN 64

On the Geomagnetic *Sd* Field.....H. MAEDA 66